

Summertime Arctic Clouds and Radiation Over SHEBA

*T. C. Benner and J. A. Curry
Program in Atmospheric and Oceanic Sciences
University of Colorado
Bolder, Colorado*

Introduction

Arctic clouds can have a substantial impact on radiative fluxes (e.g., Curry et al. 1996) and heating rates. Inhomogeneous clouds, in particular, can have very complicated effects. In the summertime arctic, these effects can be compounded by the highly reflecting yet inhomogeneous surface, with its intermingled ice, melt ponds, and open water. Numerous studies have emphasized the need for a more thorough understanding of the radiative effects of inhomogeneous clouds, while others have assessed the accuracy of common radiative transfer approximations, such as the Independent Pixel Approximation (IPA) (e.g., Cahalan et al. 1994) and the Plane Parallel Approximation (PPA), under specific conditions. This study used data from Surface Heat Budget of the Arctic Ocean (SHEBA) and FIRE-ACE (First ISCCP [International Satellite Cloud Climatology Project] Regional Experiment-Aerosol Characterization Experiment) with the Spherical Harmonics Discrete Ordinate Method (SHDOM) radiative transfer model to investigate the effects of cloud and surface inhomogeneity on radiative fluxes and heating rates in the arctic, as well as the accuracy of common radiative transfer approximations in this environment.

Data/Model Inputs

Data obtained during SHEBA and FIRE-ACE in July 1998 provided the inputs for the radiative transfer simulation. First, cloud properties were derived from microphysical measurements taken by the Gerber PVM probe, mounted on the National Center for Atmospheric Research (NCAR) C-130 aircraft. Conditions on July 21 featured a low-lying liquid cloud layer, which had pronounced east-west variability but was mostly uniform in the north-south direction. This uniformity allowed the reconstruction of a two-dimensional (2-D) (x-z) liquid water content (LWC) field from measurements taken during one profile and one transect above the SHEBA camp. Figure 1 shows this LWC field, with the corresponding optical depth field. The omission of the y dimension allowed considerable size (26 km) and high-resolution (100 m) in the x direction and high-resolution (10 m) in the z direction, due to computer memory considerations. The LWC field shows substantial horizontal variability, although it varies smoothly in the vertical.

Second, surface properties were derived from multiple sources and modeled with the same horizontal resolution as the cloud layer. Statistics for fractional coverage of open water and melt ponds were derived from downward-looking video from the C-130 (Tschudi et al. 1999). These statistics came from July 18, which was clear enough for surface mapping and temporally close to July 21. Melt ponds were

generally smaller than the horizontal grid size, so each surface grid cell was modeled as either open water or as some mixture of ice and melt pond, with the appropriate aggregate albedo and emissivity. The albedos of these components were average values measured at the camp, while the total albedo matched the measured large-scale albedo. Figure 2 shows the distribution of melt pond fraction.

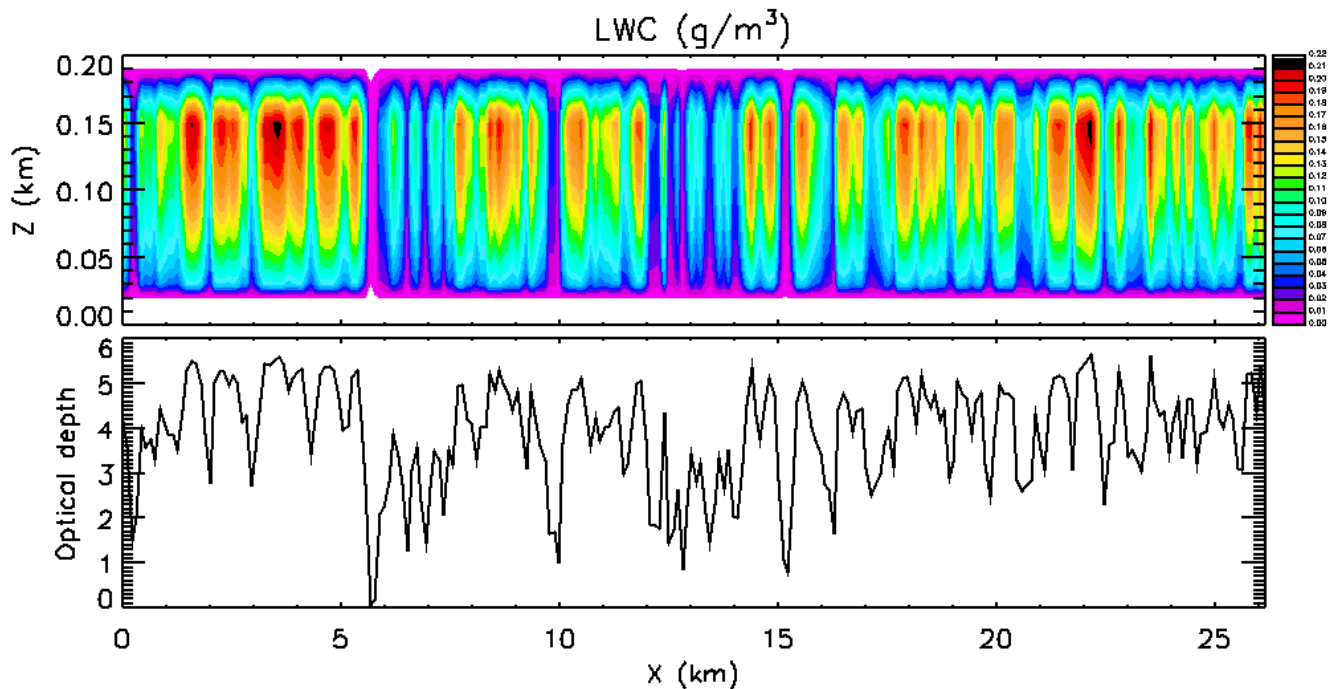


Figure 1. 2-D LWC field derived from C-130 data, with resulting horizontal distribution of optical depth.

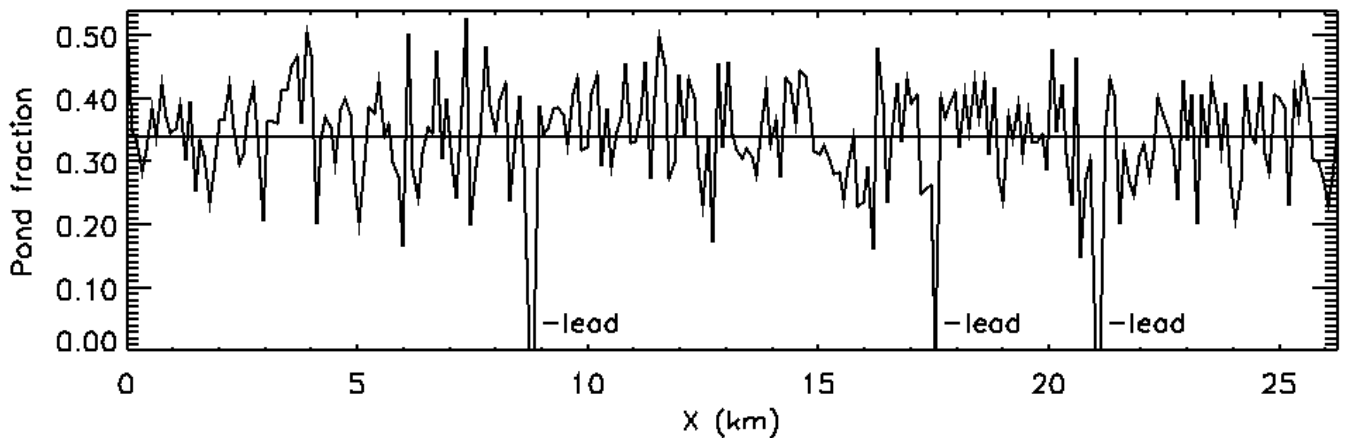


Figure 2. Horizontal distribution of melt pond fraction, using statistics derived from C-130 video.

Third, atmospheric properties were derived from direct C-130 measurements up to 6 km, with a McClatchey standard arctic summer atmosphere above. These included temperature, pressure, humidity, and ozone concentration. These atmospheric profiles extended to 25 km, i.e., far above the cloud layer, to properly account for molecular scattering (solar) and absorption (longwave). In this case, the lower atmosphere and the surface were all at about 272 K, with a strong inversion above the cloud layer.

Radiative Transfer

This study used the SHDOM radiative transfer model (Evans 1998) with all of the data inputs described above. Cloud optical properties, including the full phase function, were computed with Mie theory. Broadband radiative transfer used a correlated k-distribution, with 6 solar and 12 longwave bands (Fu and Liou 1992). Molecular scattering and absorption were also included. This model was run many times to examine different sensitivities. It was run with different surface characterizations: fully varying surface properties, a uniform surface, a totally absorbing black surface ($\alpha = 0$), and a totally reflecting white surface ($\alpha = 1$). It was also run using different radiative transfer methods: full 2-D radiative transfer; the IPA, using independent columns in x ; and the PPA, averaging over all columns in x . For each of these 12 cases, the upwelling flux above the cloud layer, the downwelling flux at the surface, and the heating rate through the cloud layer were all computed, summing over bands for both solar and longwave. More model runs produced fluxes for cases without clouds and without molecular absorption, for comparison to the fully inhomogeneous base case.

Results

Table 1 lists the solar fluxes averaged horizontally over the entire domain, for the different surface characterizations and radiative transfer methods. The small difference between the 2-D and PPA fluxes indicates that cloud inhomogeneity has little effect on the domain-average solar fluxes for any given surface characterization. Surface inhomogeneity also has little effect on the domain-average solar fluxes, assuming the total albedo is correct. As demonstrated by the extreme black and white cases, however, an incorrect surface albedo can produce significant errors. IPA and PPA produce only small errors compared to full 2-D radiative transfer.

Figure 3 shows the horizontal distribution of solar fluxes. The left-hand panels compare the three radiative transfer methods for an inhomogeneous surface. Despite the similar domain-average fluxes, there are significant local variations. The effects of leads and cloud variability are readily apparent. Both IPA and PPA introduce large local errors. The right-hand panels compare the four surface characterizations for 2-D radiative transfer. Surface inhomogeneity produces some flux variability, especially in the upward flux above a lead, but in general the difference is not large. However, errors in total albedo produce a very large bias, as shown by the $\alpha = 0$ and $\alpha = 1$ cases.

Table 1. Domain-average solar fluxes (W/m^2) above and below the cloud layer, for the four surface characterizations and the three radiative transfer methods. Values in red are percent errors of radiative transfer approximations compared to 2-D radiative transfer.

		Surface Type			
		Variable	Uniform	Black ($a = 0$)	White ($a = 1$)
2D	Up	330.5	330.1	174.3	580.2
	Down	454.8	454.9	398.9	545.7
IPA	Up	331.5 +0.3 %	330.9 +0.2 %	174.1 -0.1 %	581.6 +0.2 %
	Down	455.8 +0.2 %	455.7 +0.2 %	400.3 +0.4 %	546.0 +0.1 %
PPA	Up	332.1 +0.5 %	332.1 +0.6 %	177.5 +1.8 %	581.0 +0.1 %
	Down	453.2 -0.4 %	453.2 -0.4 %	396.8 -0.5 %	544.2 -0.3 %

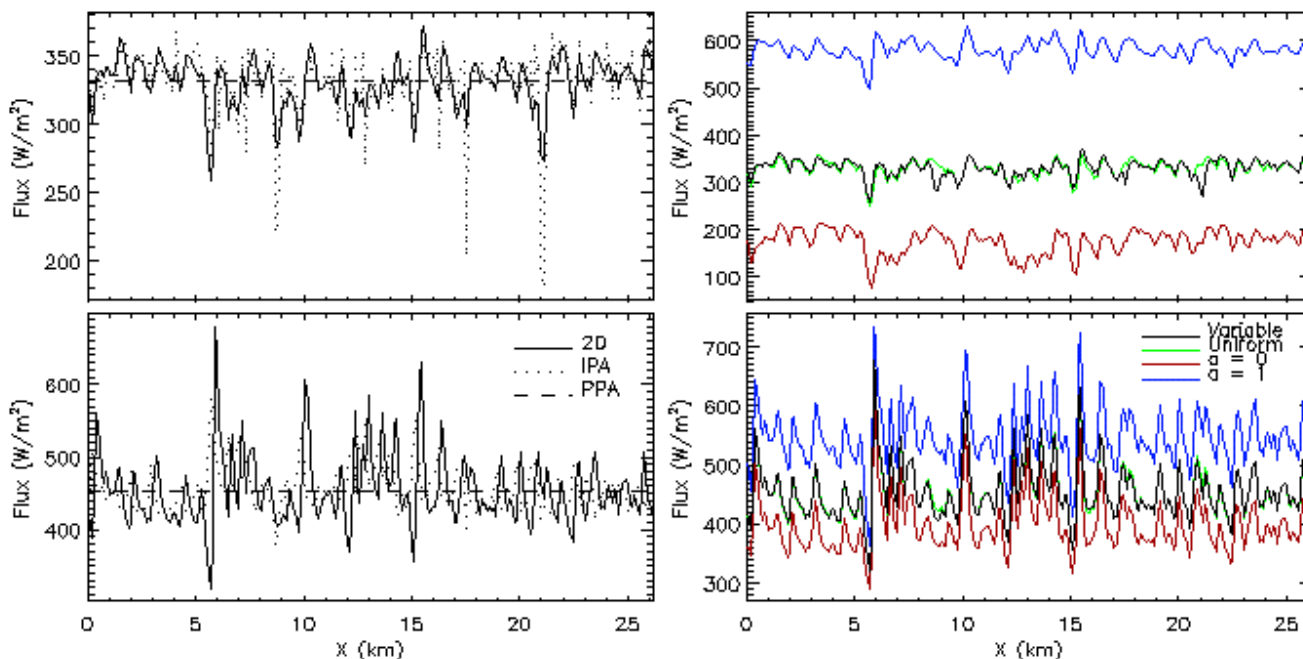


Figure 3. Horizontal distribution of solar fluxes, comparing radiative transfer methods (left) and surface types (right).

Also computed, but not shown, was a comparison of solar fluxes for model runs with and without clouds. Despite being relatively optically thin, this cloud layer produces a total solar forcing at the surface of -133 W/m^2 , which is 23% of the clear-sky value. It produces a total solar forcing of $+60 \text{ W/m}^2$ (22%) above the cloud layer.

Table 2 lists the domain-average longwave fluxes, for the different surface characterizations and radiative transfer methods. Cloud inhomogeneity has little effect on the domain-average longwave fluxes for any given surface characterization, and surface inhomogeneity has essentially no effect. IPA and PPA produce only small errors compared to full 2-D radiative transfer. However, the surface and the cloud layer were all at about 272 K, which served to make the fluxes very uniform. One would expect greater temperature variability to allow larger errors.

Table 2. Domain-average longwave fluxes (W/m^2) above and below the cloud layer, for variable and uniform surface, and the three radiative transfer methods. Values in red are percent errors of radiative transfer approximations compared to 2-D radiative transfer.

		Surface Type	
		Variable	Uniform
2-D	Up	309.5	309.5
	Down	295.9	295.9
IPA	Up	309.5 --	309.5 --
	Down	295.4 -0.2 %	295.4 -0.2 %
PPA	Up	309.4 --	309.4 --
	Down	297.1 +0.4 %	297.1 +0.4 %

Figure 4 shows the horizontal distribution of longwave fluxes. The left-hand panels compare the three radiative transfer methods for a fully inhomogeneous surface. IPA produces local errors of up to 5%, especially in downward fluxes under thin parts of the cloud layer. There is little impact on upward fluxes above the cloud layer, which are highly uniform due to the small temperature variability. The right-hand panels compare the base case to model runs without clouds and without gaseous absorption. The cloud layer produces a total longwave forcing at the surface of 36 W/m^2 , which is 15% of the clear-sky value. Molecular absorption and emission smooth the radiation field to a large extent. Omitting them produces excess variability and a substantial bias - 32 W/m^2 at the surface. In this case, emission from the inversion above the cloud layer increases the downwelling longwave flux at the surface. More model runs also compared longwave fluxes with different surface characterizations, for 2-D radiative transfer (not shown). Surface inhomogeneity has little impact on fluxes, due to the uniform surface temperature and near-uniform surface emissivity of this summertime case.

Modeled downwelling fluxes were also compared to those measured at the SHEBA camp by the Atmospheric Radiation Measurement (ARM) Precision Spectral Pyranometer (solar) and Precision Infrared Radiometer (longwave) instruments, using one hour of data around the same time as the cloud

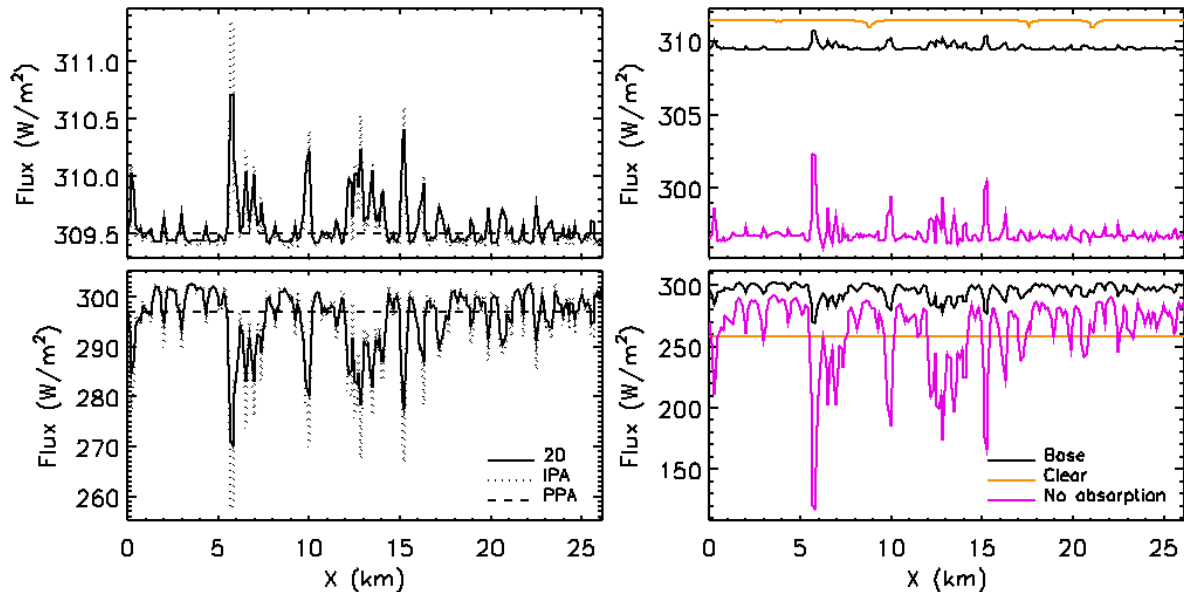


Figure 4. Horizontal distribution of longwave fluxes, comparing radiative transfer methods (left) and effects of clouds and molecular absorption (right).

measurements from the C-130 data. Compared to these measured fluxes, the best modeled mean fluxes (see Tables 1 and 2) are in error by only 5% for solar and 1% for longwave. This confirms reasonable accuracy in the retrievals and the radiative transfer simulation.

Figure 5 shows the domain-average solar heating rate profile through the cloud layer, comparing radiative transfer methods and surface characterizations. As expected, the heating rate is greatest in the highest, thickest part of the cloud layer, which receives the most solar radiation. There is also significant heating in the lower part of the cloud layer, however, some of which results from upwelling radiation from the highly reflecting surface. IPA and PPA introduce only a few percent errors at any altitude. Surface inhomogeneity has no effect on the solar heating rate, as long as the total albedo is correct. The domain-average longwave heating rate (not shown) is similarly influenced. IPA and PPA introduce errors up to about 5% in the thickest part of the cloud top, and surface inhomogeneity has essentially no effect. Despite the small variation of these domain-average heating rates, however, the inhomogeneities still induce local variations, which may be important for turbulent kinetic energy production.

Summary and Future Work

We have used data from SHEBA and FIRE-ACE with the SHDOM radiative transfer model to examine radiative fluxes and heating rates in the arctic. Cloud inhomogeneity strongly affects the spatial variability of solar fluxes above and below the cloud layer and of longwave fluxes below. However, it has only a small impact on domain-average fluxes (< 2%). Surface inhomogeneity also affects the spatial variability of solar fluxes, but not longwave fluxes (although the cloud and the surface in this

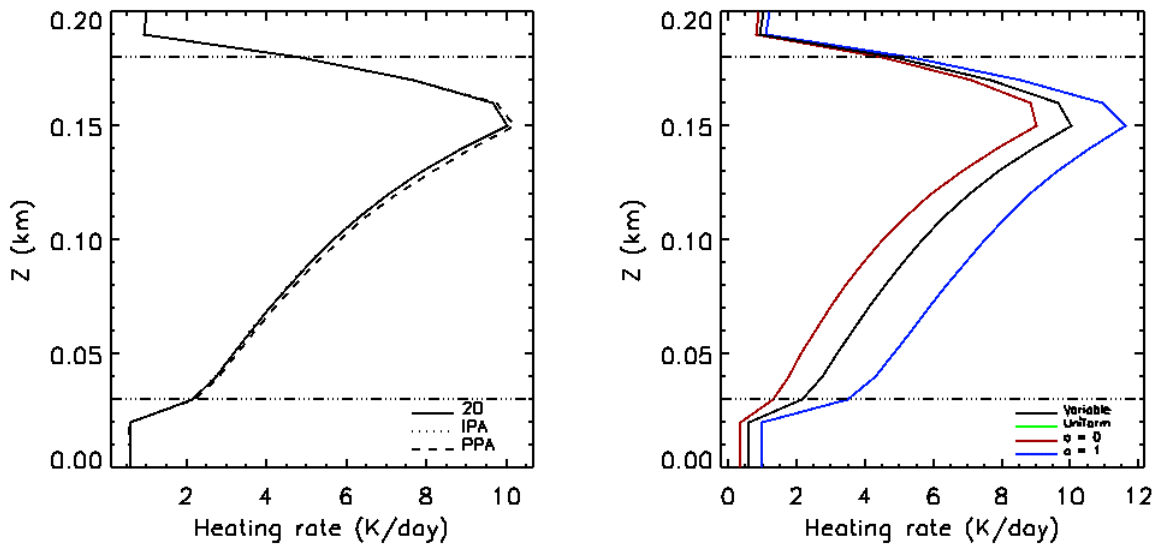


Figure 5. Domain-average solar heating rates, comparing radiative transfer methods (left) and surface types (right).

case were all at about 272 K). However, it has little impact on domain-average solar fluxes ($< 0.2\%$) and heating rates ($\sim 0\%$), assuming the domain-average albedo has been correctly specified. IPA and PPA create only minor errors in domain-average fluxes ($< 2\%$) and heating rates ($< 6\%$) for a given surface characterization. Overall, the clouds have a substantial impact on solar and longwave fluxes, both upward and downward. Gaseous absorption has a noticeable impact on local and domain-average longwave fluxes. The best modeled fluxes are generally close to measured fluxes. In the future we will examine a greater variety of cloud cases and data sources to more fully explore the effects of spatial variability in arctic clouds.

References

- Cahalan, R. F., W. Ridgeway, W. J. Wiscombe, T. L. Bell, and J. B. Snider, 1994: The albedo of fractal stratocumulus clouds. *J. Atmos. Sci.*, **51**, 2434-2455.
- Curry, J. A., W. B. Rossow, D. Randall, and J. L. Schramm, 1996: Overview of arctic cloud and radiation characteristics. *J. Climate*, **9**, 1731-1764.
- Evans, K. F., 1998: The spherical harmonics discrete ordinate method for three-dimensional radiative transfer. *J. Atmos. Sci.*, **55**, 429-446.
- Fu, Q., and K. N. Liou, 1992: On the correlated k-distribution method for radiative transfer in inhomogeneous atmospheres. *J. Atmos. Sci.*, **49**, 2139-2156.
- Tschudi, M. A., J. A. Curry, and J. A. Maslanik, 1999: Airborne observations of surface features during SHEBA. *5th Conf. on Polar Meteorology and Oceanography*, Dallas, Texas, Amer. Meteor. Soc., 162-165.